

# Programmatic Imitation Learning from Unlabeled and Noisy Demonstrations

Jimmy Xin, Linus Zheng, Jiayi Wei, Kia Rahmani, Jarrett Holtz, Isil Dillig, and Joydeep Biswas  
Department of Computer Science, The University of Texas at Austin

**Abstract**—Imitation Learning (IL) is a promising paradigm for teaching robots to perform novel tasks using demonstrations. Most existing approaches for IL utilize neural networks (NN), however, these methods suffer from several well-known limitations: they 1) require large amounts of training data, 2) are hard to interpret, and 3) are hard to repair and adapt. There is an emerging interest in *programmatic imitation learning* (PIL), which offers significant promise in addressing the above limitations. In PIL, the learned policy is represented in a programming language, making it amenable to interpretation and repair. However, state-of-the-art PIL algorithms assume access to action labels and struggle to learn from noisy real-world demonstrations. In this paper, we propose PLUNDER, a novel PIL algorithm that integrates a probabilistic program synthesizer in an iterative Expectation-Maximization (EM) framework to address these shortcomings. Unlike existing PIL approaches, PLUNDER synthesizes *probabilistic* programmatic policies that are particularly well-suited for modeling the uncertainties inherent in real-world demonstrations. Our approach leverages an EM loop to simultaneously infer the missing action labels and the most likely probabilistic policy. We benchmark PLUNDER against several established IL techniques, and demonstrate its superiority across five challenging imitation learning tasks under noise. PLUNDER policies achieve 95% accuracy in matching the given demonstrations, outperforming the next best baseline by 19%. Additionally, policies generated by PLUNDER successfully complete the tasks 17% more frequently than the nearest baseline.

## I. INTRODUCTION

Imitation Learning (IL) is a popular approach for teaching robots how to perform novel tasks using only human demonstrations, without the need to specify a reward function or a system transition function [1]. Most current IL approaches use neural networks to represent the learned policy, mapping the agent’s state to actions. While effective, these approaches have several well-known limitations: 1) they require large amounts of training data, 2) they are hard to interpret, and 3) they are hard to repair and adapt to novel settings. Seeking to address these limitations, *programmatic imitation learning* (PIL) approaches synthesize *programmatic policies* from demonstrations, which are human-readable, require significantly fewer demonstrations, and are amenable to repair and adaptation [2], [3], [4], [5].

However, existing PIL methods require *action labels* for human demonstrations, which are often unavailable in real-world settings. Furthermore, these methods assume that the demonstrations are *nearly noise-free*, which is rarely the case in practice. In this paper, we introduce two key insights to address the above challenges. First, given human demonstrations without action labels, inferring the action labels is a *latent variable estimation* problem. Second, instead of

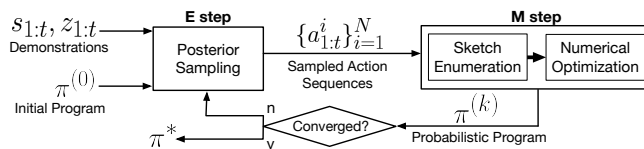


Fig. 1: Overview of PLUNDER

synthesizing a deterministic policy, synthesizing a *probabilistic* policy allows us to model the uncertainties inherent in real-world demonstrations. Combining these insights, we introduce PLUNDER<sup>1</sup>, a new PIL algorithm that synthesizes *probabilistic programmatic policies* from unlabeled and noisy demonstrations.

Figure 1 presents an overview of PLUNDER. The algorithm starts with an initial randomized policy ( $\pi^{(0)}$ ) and iteratively improves this policy while also improving its estimates of the action labels using an Expectation-Maximization (EM) algorithm [6]. In the E step, PLUNDER samples posterior action label sequences by combining the current policy with the given demonstrations. In the M step, it synthesizes a new policy that maximizes the likelihood of producing actions that match the previously sampled action labels. To improve the scalability of the M step, we also propose an incremental synthesis technique that narrows the search on policies similar to the best policy found in the previous iteration. This process is repeated until convergence, yielding jointly an optimal policy  $\pi^*$  and the most likely action labels for the demonstrations.

To evaluate our approach, we apply PLUNDER to five standard imitation learning tasks and compare the results with multiple baselines, including three state-of-the-art IL techniques. We empirically show that PLUNDER synthesizes policies that conform to the demonstrations with 95% accuracy, which is 19% higher than the next best baseline. Furthermore, PLUNDER’s policies are 17% more successful than the closest baseline in completing the tasks. We also present case studies showing the advantages of PLUNDER, including resilience to noise, scalability to complex probabilistic programs, and interpretability to the end user. Our implementation of the PLUNDER algorithm is available as an open-source library (<https://github.com/ut-amrl/plunder>).

## II. PROBLEM FORMULATION

Given a set of demonstrations of a task, the PIL problem addressed in this paper is to infer a probabilistic *Action*

<sup>1</sup>Policy Learning from Unlabeled Noisy DEMonstrations for Robots

*Selection Policy (ASP)* that is maximally consistent with the given demonstrations and that captures the behavior intended by the demonstrator.

In particular, we consider learning policies over a continuous state space  $S$  (e.g.,  $\mathbb{SE}(2)$  for a ground mobile robot) and a discrete action space  $A$ , where the actions are abstracted as *skills* [7], [8]. For instance, an autonomous vehicle may have skills such as accelerate (**ACC**), decelerate (**DEC**), and maintain constant velocity (**CON**). A probabilistic ASP,  $\pi$ , is a probabilistic program that, given the agent’s current state ( $s_i \in S$ ) and its current action ( $a_i \in A$ ), defines the probability of taking the next action  $a_{i+1} \sim \pi(s_i, a_i)$ .

The given demonstrations consist of an agent’s *observation* trajectories,  $z_{1:t}$  (e.g., the vehicle’s acceleration input), and the corresponding *state* trajectories,  $s_{1:t}$  (e.g., the vehicle’s velocity), but do not include any action labels. Our objective is to infer a *maximum a posteriori (MAP)* estimate of an ASP  $\pi^*$  as follows:

$$\pi^* = \arg \max_{\pi} P(z_{1:t}, \pi | s_{1:t}) \quad (1)$$

$$= \arg \max_{\pi} P(z_{1:t} | s_{1:t}, \pi) P(\pi) \quad (2)$$

We introduce action labels,  $a_{1:t}$ , as marginalized latent variables which should be estimated jointly with the ASP:

$$\pi^* = \arg \max_{\pi} \sum_{a_{1:t}} P(z_{1:t} | a_{1:t}, s_{1:t}) P(a_{1:t} | s_{1:t}, \pi) P(\pi) \quad (3)$$

In the above formula  $P(z_{1:t} | a_{1:t}, s_{1:t})$  is the *observation model* that defines the likelihood of an observation trajectory given the agent’s actions and states, and  $P(a_{1:t} | s_{1:t}, \pi)$  is defined by the policy  $\pi$ . We also make the Markov assumptions on ASPs and the observation model, i.e.,

$$P(a_{1:t} | s_{1:t}, \pi) = \prod_{i=1}^t P(a_i | a_{i-1}, s_i, \pi), \quad (4)$$

$$P(z_{1:t} | a_{1:t}, s_{1:t}) = \prod_{i=1}^t P(z_i | a_i, s_i), \quad (5)$$

yielding our final objective,

$$\pi^* = \arg \max_{\pi} \sum_{a_{1:t}} \prod_{i=1}^t P(z_i | a_i, s_i) P(a_i | a_{i-1}, s_i, \pi) P(\pi). \quad (6)$$

There are two major challenges in solving (6). First, directly computing the sum over all action trajectories is computationally intractable. Second, the search space for probabilistic policies is prohibitively large, making any naïve search within this space unscalable. In section III, we explain our approach to overcome both of these challenges in a tractable manner.

#### A. Example: Stop-Sign

Consider an autonomous vehicle that is required to drive on a straight road and make appropriate stops at every stop sign. Defining a reward function or an objective function that accurately captures the desired behaviors for executing this task is challenging. Instead, we aim to learn an ASP from expert demonstrations of the task using imitation learning.

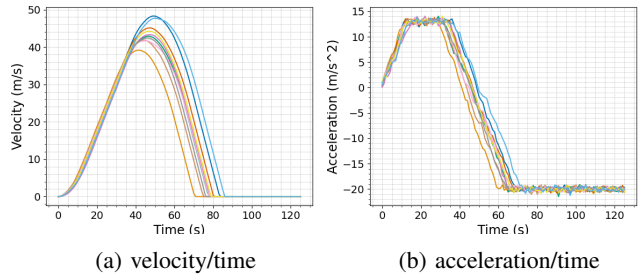


Fig. 2: Demonstration trajectories for the Stop Sign task. The acceleration value of this particular vehicle cannot exceed  $a_{\max} \approx 13m/s^2$  or drop below  $a_{\min} \approx -20m/s^2$ .

Figure 2 presents 10 demonstrations for this task. Each demonstration consists of the vehicle’s velocity and acceleration trajectories between two consecutive stop signs. Observe the variations in different executions of this maneuver. For instance, some demonstrations prefer a more gradual acceleration and deceleration for a comfortable ride. In contrast, others showcase harder acceleration and deceleration.

As we will discuss in the subsequent sections, the PLUNDER algorithm is capable of reasoning about variations and noise in demonstrations and can synthesize a probabilistic ASP that captures the behavior intended by the demonstrations collectively.

---

#### Algorithm 1 The PLUNDER Algorithm

---

**Inputs:** state trajectories:  $\bar{S}$ , observation trajectories:  $\bar{Z}$ , observation model:  $O$ , initial policy:  $\pi^{(0)}$ , convergence threshold:  $\gamma$   
**Output:** probabilistic action selection policy:  $\pi^*$

```

1:  $k = 0$ 
2: while  $\text{likelihood}(\bar{S}, \bar{Z}, O, \pi^{(k)}) \leq \gamma$  do
3:    $\{a_{1:t}^i\}_{i=1}^N := \text{runPF}(\bar{S}, \bar{Z}, O, \pi^{(k)})$  // E step
4:    $\pi^{(k+1)} := \text{synthesize}(\pi^{(k)}, \bar{S}, \{a_{1:t}^i\}_{i=1}^N)$  // M step
5:    $k = k + 1$ 
6: end while
7: return  $\pi^{(k)}$ 

```

---

### III. THE PLUNDER ALGORITHM

Algorithm 1 provides an overview of our Expectation-Maximization (EM) approach, which is designed to tractably approximate the MAP estimate in equation (6). The inputs to the algorithm are a set of  $D$  demonstrations consisting of state trajectories ( $\bar{S} := \{s_{1:t}^i\}_{i=1}^D$ ) and observation trajectories ( $\bar{Z} := \{z_{1:t}^i\}_{i=1}^D$ ), the observation model  $O$ , the initial policy  $\pi^{(0)}$ , and a threshold,  $\gamma$ , for determining whether the synthesized policy has converged.

The algorithm alternates between the E step (line 3) and the M step (line 4). In the E step, a posterior sampling of  $N$  action label trajectories is performed using the current candidate ASP  $\pi^{(k)}$  and the given demonstration trajectories. These sampled action trajectories are then used in the M step to synthesize a policy that is maximally consistent with those action trajectories. After each iteration of the E and M steps, the likelihood of the synthesized policy’s prediction on the given trajectories is measured. Once the desired likelihood is

$c$	$\in$	$\{a_{\min}, a_{\max}, v_{\max}, \dots\}$	(domain constants)
$y$	$\in$	$\{v, acc, d_{\text{stop}}, \dots\}$	(domain variables)
$a$	$\in$	$\{\text{ACC}, \text{DEC}, \text{CON}\}$	(domain actions)
$g$	$\in$	$\{+, -, \times, \text{distTrv}, \text{timeToStp}, \dots\}$	(domain functions)
$r$	$\in$	$\mathbb{R}$	(ASP parameters)
$f$	$:=$	$y \mid c \mid g(f_1, \dots, f_n)$	(features)
$\phi_{a,a'}$	$:=$	$\text{true} \mid \text{false} \mid \phi_1 \wedge \phi_2 \mid \phi_1 \vee \phi_2$ $\mid \text{randSwitch}(r) \mid \text{flp}(\text{lgS}(f, r_1, r_2))$	(conditions)

Fig. 3: Probabilistic domain-specific language. Top four productions are specific to the example in subsection II-A.

reached (*i.e.*, the policy has converged), the algorithm outputs the latest synthesized policy as its final result,  $\pi^*$ .

In the remainder of this section, we introduce the syntax of probabilistic ASPs synthesized in PLUNDER, and present further details about the E and M steps of Algorithm 1.

### A. Probabilistic ASPs

In our setting, the set of agent’s actions,  $A$ , is both discrete and finite. Therefore, at each time step, the policy must decide on the next action to take from this set. This decision is conditioned on the agent’s last action and state; thus, the logic of policy  $\pi$  can be defined using a set of binary *transition conditions*  $\Phi := \{\phi_{a,a'} \mid a, a' \in A\}$ , where each  $\phi_{a,a'}$  is evaluated on the agent’s state. If the agent takes action  $a$  at time  $t$  and  $\phi_{a,a'}$  holds true on the current state, then the agent will take action  $a'$  at time  $t + 1$ . The policy also maintains an order among transition conditions and uses it to break ties when multiple conditions are true.

Since we want to synthesize probabilistic policies, each transition condition  $\phi_{a,a'}(\cdot)$  is defined in a probabilistic Domain-Specific Language (pDSL) [9], [10], where Boolean expressions in each state are evaluated to `true` with a certain probability. Figure 3 presents the pDSL used in PLUNDER. The numerical expressions in this pDSL are domain-specific and capture the physical properties of the system.

Boolean conditions are captured using the probabilistic coin-flip function, `flp`( $p$ ), which evaluates to `true` with probability  $p$  and evaluates to `false` otherwise. Within this coin-flip function, the S-shaped logistic function, `lgS`, is used to approximate numerical inequalities. For instance, the deterministic inequality  $e > x_0$  can be transformed into a probabilistic inequality `flp`(`lgS`( $f, x_0, k$ )). Here, `lgS`( $f, x_0, k$ ) maps the difference between  $f$  and  $x_0$  to a value in the range  $(0, 1)$  in a smooth and continuous fashion. The parameter  $k$  controls the growth rate of the logistic curve. A larger value of  $k$  indicates sharper growth, leading to less uncertainty in the probabilistic inequality.

Lastly, the function `randSwitch`( $r$ ) dictates that the policy retains the current action with probability  $1 - r$  or transitions to another randomly selected action with probability  $r$ . This function is stochastic, however, it embodies the “*action inertia*” heuristic, suggesting that useful policies avoid switching between actions too frequently.

### B. Expectation (E) Step

During the E step (line 3) of Algorithm 1, the current estimate of the ASP,  $\pi^{(k)}$ , is used to sample  $N$  plausible

action sequences from the posterior distribution  $\{a_{1:t}^i\}_{i=1}^N \sim P(\cdot \mid s_{1:t}, z_{1:t}, \pi^{(k)})$ . This posterior sampling problem is particularly amenable to inference using Monte-Carlo estimation algorithms [11], and we use a *particle filter* [12] to sample a policy’s action label sequences.

The function `runPF`( $\bar{S}, \bar{Z}, O, \pi^{(k)}$ ) implements the particle filter as follows. For each state trajectory  $s_{1:t} \in \bar{S}$ , the function utilizes  $\pi^{(k)}$  to sample action labels forward in time. Next, it employs the observation model  $O$  to re-weight and re-sample the particles. This ensures that sequences more aligned with the provided observations have a higher likelihood of duplication and representation in the final sample set. After completing this procedure for all provided demonstrations, the final particle set represents  $\{a_{1:t}^i\}_{i=1}^N$ , *i.e.*,  $N$  plausible action label sequences given the current policy and the demonstration traces.

### C. Maximization (M) Step

During the M Step (line 4) of Algorithm 1, a new ASP is synthesized using the function `synthesize`( $\cdot$ ). This function, given the state trajectories  $\bar{S}$  and the sampled action sequences from the previous E step  $\{a_{1:t}^i\}_{i=1}^N$ , aims to solve the following objective:

$$\pi^{(k+1)} = \arg \max_{\pi \in \mathbb{N}(\pi^{(k)})} \sum_{i=1}^N \log P(a_{1:t}^i \mid s_{1:t}, \pi) + \log P(\pi) \quad (7)$$

The above formula indicates that the synthesized policy should be as consistent as possible with the sampled action sequences and should have a high probability of occurrence based on the ASP prior. We define the ASP prior as  $\log P(\pi) = -\lambda \cdot \text{size}(\pi)$ , where  $\lambda \geq 0$  is a hyperparameter. This prior disincentivizes synthesizing structurally complex programs such as programs with case-based reasoning that over-fit to inputs.

The function `synthesize`( $\cdot$ ) implements a bottom-up inductive synthesizer [13], where the production rules described in Figure 3 are used to enumerate a set of policy structures, or *sketches* [14]. The enumeration begins with the set of numerical features – consisting of constants, variables, and function applications – which are used to construct probabilistic threshold sketches with two unknown parameters. The threshold sketches are combined using disjunctions and conjunctions to construct the final set of policy-level sketches.

Each policy sketch can be converted into a complete policy by determining the unknown real-valued parameters in the probabilistic thresholds. Our goal is to identify the parameters that optimize the objective given by equation (7). To solve this optimization problem, we employ the Line Search Gradient Descent (L-BFGS) algorithm [15], selecting the top result out of four random initial assignments. After completing all sketches, the `synthesize`( $\cdot$ ) function returns the optimal policy according to (7) as its final output.

While the above inductive synthesis approach is guaranteed to find the optimal solution within its bounded search space, enumerating programs this way rapidly becomes intractable. This is especially problematic in our setup, where

the synthesis is integrated within the EM loop, which might need many iterations to converge. To address this challenge, we restrict the search space for  $\pi^{(k+1)}$  to  $\mathcal{N}(\pi^{(k)})$ , the *syntactic neighbourhood* of  $\pi^{(k)}$ . To enumerate the syntactic neighborhood of a policy, we mutate its abstract syntax tree to derive a set of new expressions. In particular, we apply the following types of mutations:

- 1) Add a new threshold predicate with a random feature.
- 2) Simplify the policy by removing an existing predicate.
- 3) Swap conjunctions with disjunctions, and vice-versa.
- 4) Augment numerical features by applying random functions with random parameters.
- 5) Simplify features by removing function applications.

Each syntactic neighbourhood, in addition to the above set of mutated expressions, contains a set of atomic features. This allows the synthesizer to “reset” to simpler policies if needed.

To further improve the scalability of the `synthesize(.)` function, we also prune the search space using a type system based on physical dimensional constraints, as previously done in [2]. This type system tracks the physical dimensions of expressions and discards those that are inconsistent.

The above two pruning methodologies significantly reduce the policy search space, allowing the `synthesize(.)` function to be tractably used within our EM framework.

#### D. Example: Stop-Sign

Figure 4 displays the results of four non-consecutive iterations of the EM loop for the Stop-Sign example. Each iteration presents  $\pi^{(i)}$ , the candidate policy synthesized during the M step, and its accuracy, alongside the corresponding action sequences sampled using the policy. Due to space constraints, we only show the conditions  $\phi_{\text{ACC,CON}}$  and  $\phi_{\text{CON,DEC}}$  for each candidate policy. These conditions represent transitions from acceleration to constant velocity, and from constant velocity to deceleration, respectively. Each sampled action sequence is depicted as a color-coded horizontal line. Specifically, **ACC** time-steps are shown in red, **CON** time-steps are shown in cyan, and **DEC** time-steps are shown in blue. Because the candidate policies are probabilistic, the sequences from the same policy exhibit random variations. However, these variations diminish as the EM loop progresses and confidence in the synthesized policy increases.

The EM loop is initiated with a trivial ASP,  $\pi^{(0)}$ , employing `randSwitch(0.1)` for all transition conditions. The algorithm then alternates between E and M Steps, progressively refining the candidate policy. This refinement continues until the desired level of accuracy is achieved in  $\pi^{(5)}$ , which is returned as the final solution for the Stop-Sign task.

In  $\pi^{(5)}$ , the transition condition  $\phi_{\text{ACC,CON}}$  specifies that the vehicle should switch from acceleration to constant velocity, as its velocity nears the recommended maximum velocity,  $v_{\text{max}}$ . Likewise,  $\phi_{\text{CON,DEC}}$  indicates that the vehicle should transition from constant speed to deceleration when the estimated stop distance based on the current speed (`distTrv`), approaches the remaining distance to the next stop sign ( $d_{\text{stop}}$ ). These probabilistic expressions intuitively

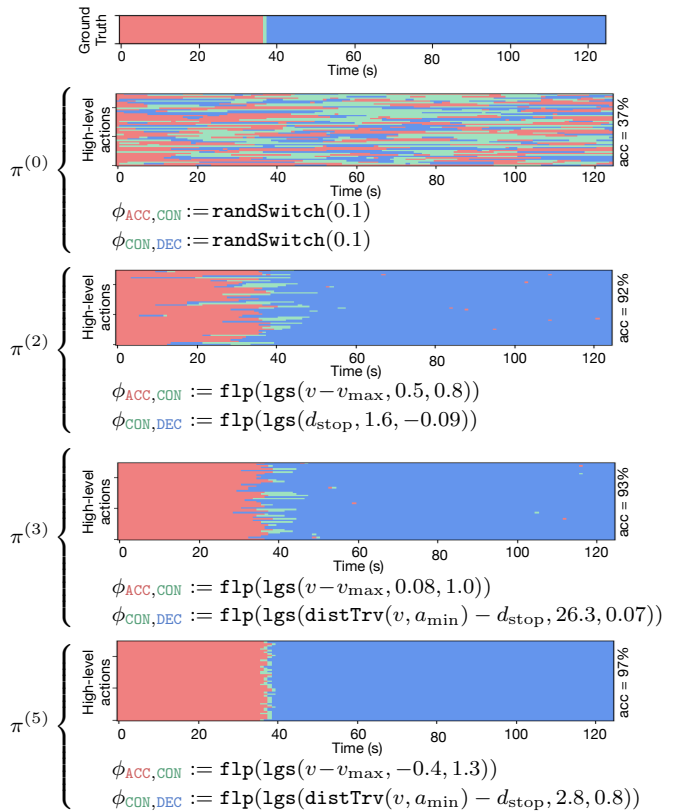


Fig. 4: Best candidate programs found at each iteration and the corresponding action sequence samples. The ground-truth sequence is shown at the top. Only  $\phi_{\text{ACC,CON}}$  and  $\phi_{\text{CON,DEC}}$  from each policy are shown due to space constraints.

encapsulate the human demonstrators’ intent for this specific task and are amenable to repair and fine-tuning [16].

Synthesizing ASPs such as  $\pi^{(5)}$ , is challenging due to their intricate structures with multiple functions, variables, and numerical constants. In the subsequent section, we will present more complex examples featuring multiple disjuncts and conjuncts drawn from our benchmarks.

## IV. EXPERIMENTAL EVALUATIONS

We evaluated our approach using five standard imitation learning tasks from two challenging environments.

**Autonomous Vehicle Environment:** We utilize the open-source simulation environment HIGHWAY-ENV [17], where the demonstrator controls the acceleration and steering of a vehicle moving on a straight multi-lane highway. We consider the following three tasks within this environment. The **Stop Sign (SS)** task is the motivating example described in previous sections and involves the demonstrator controlling the vehicle’s acceleration in order to move to and stop at target locations. The **Pass Traffic (PT)** task is more complex and involves ongoing traffic. In this task, the agent’s goal is to switch lanes quickly and safely to pass slower traffic. Finally, in the **Merge (MG)** task, the vehicle starts in the leftmost lane, and the expected behavior is to merge into the rightmost lane without colliding with the moving traffic.

**Robotic Arm Environment:** We also use the open-source PANDA-GYM framework [18] that simulates a multi-joint robotic arm. Within this environment, the demonstrator manages both the end effector’s movement in three-dimensional space and the signal to control its grip. We evaluate our approach using two tasks defined in this environment. The first is the **Pick and Place (PP)** task, which requires the arm to grab an object and then move it to a designated location. The second is the **Stack (ST)** task, which is more complex and requires stacking two boxes on top of each other in the correct order.

For each of the above five tasks, we generated a set of demonstrations (*i.e.*, state and observation trajectories) using a ground-truth policy that we implemented manually. In addition to the *transition noise* caused by the probabilistic nature of the ground-truth policies, the generated trajectories were also perturbed with additional Gaussian *actuation noise*. Presence of actuation noise makes the policy-inference task more realistic, as such noise is commonly encountered when obtaining demonstrations in the real world. The demonstrations for each task were divided into a training set and a test set. Figure 2 presented the training set for the SS task.

#### A. Baselines

We compare the performance of PLUNDER against five baselines, including three state-of-the-art IL approaches.

**Greedy:** Our first baseline represents a straightforward solution to the problem of imitation learning from unlabeled trajectories, where each time step is greedily labeled with the action whose likelihood is highest according to the observation model. The same policy synthesizer as PLUNDER’s M step is then applied on these greedily labeled trajectories.

**OneShot:** The next baseline synthesizes a policy from labels sampled using a particle filter and the  $\pi^{(0)}$  policy. This method can be viewed as the first iteration of PLUNDER, except it does not employ incremental synthesis, and instead directly searches over a larger program space in one shot.

**LDIPS:** Our third baseline is LDIPS [2], a state-of-the-art PIL approach which synthesizes a policy via sketch enumeration and a reduction to satisfiability modulo theories (SMT). Unlike PLUNDER, LDIPS does not account for noise in the demonstrations and generates only deterministic policies. Furthermore, LDIPS requires action labels for synthesizing a policy. For this, we use the same action labels given to the OneShot baseline.

**BC/BC+:** The next baseline (BC) implements Behavior Cloning [19], a well-established imitation learning technique. We trained an LSTM with 64 hidden units to predict the next observation conditioned on all previous states and observations. BC+ extends the BC baseline by incorporating access to action labels and the observation model. In BC+, rather than predicting observations directly, the LSTM outputs a distribution over the available action labels. The observations are then predicted by performing a weighted sum based on the output of the observation model for each action label.

**GAIL:** Our final baseline is GAIL, another state-of-the-art method for imitation learning from expert trajectories [20].

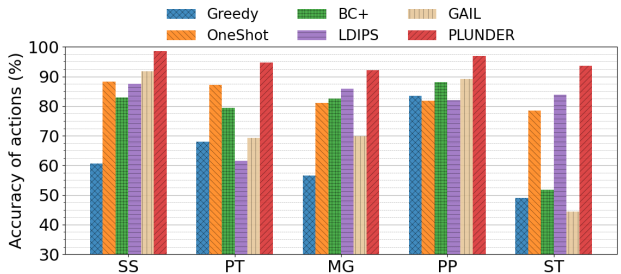


Fig. 5: Accuracy of Action Labels

	SS	PT	MG	PP	ST	avg
Greedy	-2.19	-2.10	-2.41	-0.51	-5.03	-2.45
OneShot	-1.12	-0.47	-1.32	-1.54	-1.64	-1.22
BC	-3.98	-0.96	-1.18	-1.92	-1.48	-1.90
BC+	-1.20	-0.70	-1.16	0.31	-2.78	-1.11
GAIL	-1.19	-1.30	-1.63	-0.28	-8.82	-2.64
LDIPS	-1.40	-2.03	-1.25	-1.75	-1.29	-1.54
PLUNDER	-0.78	0.37	-0.89	0.59	-0.96	-0.33

Fig. 6: Log-Likelihood of Observations

GAIL employs both a generator network and a discriminator network, using the principles of Generative Adversarial Networks (GANs) [21]. Details of our setup for GAIL and hyperparameters used for training are available in PLUNDER’s online repository.

#### B. Alignment with Demonstrations

We evaluate the ability of PLUNDER and the baselines to learn a policy that closely mimics the demonstrations in the training set. Figure 5 presents the accuracy of action labels each learned policy produces on the test trajectories. BC is excluded because it does not produce action labels. The results reveal that PLUNDER consistently outperforms all other baselines, achieving an average accuracy of 95%. We observe that the Greedy approach performs particularly poorly because of its tendency to over-fit to noise. The results confirm that utilizing a particle filter for inferring action labels, as implemented in the OneShot baseline, yields better performance compared to the naïve Greedy approach. We also find that the performance of LDIPS is significantly lower than that of PLUNDER, confirming that deterministic policies are insufficient for capturing uncertainties present in the given demonstrations.

We also report the log-likelihood of observations generated by each policy in Figure 6. Again, across all evaluated tasks, PLUNDER exhibits superior performance, yielding the highest log-likelihood.

Figure 7 visualizes samples of the ground-truth trajectories (in green) and the corresponding trajectories generated by the PLUNDER policy (in orange). The trajectories synthesized by PLUNDER closely align with the ground-truth across all benchmarks. Due to space limitations, we include a subset of observations from each task; however, we witnessed similar behaviors across all observations.

#### C. Task Completion Rate

We next evaluate the success rate of the learned policies using PLUNDER and other baselines. Each learned policy was

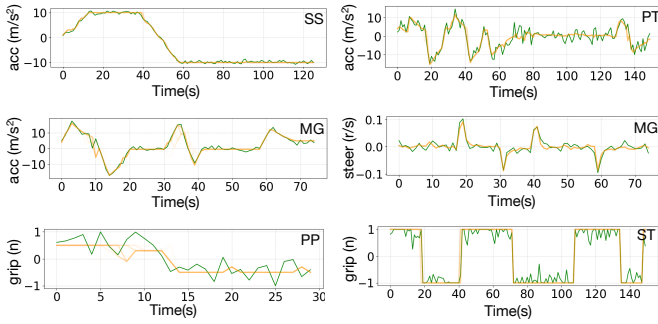


Fig. 7: Observation trajectories from the ground-truth policy (green line) and the PLUNDER policy (orange line).

executed 100 times on randomly initialized environments and we report the percentage of executions where the task was successfully completed. The results are presented in Figure 8. Notably, PLUNDER achieves an average success rate of 90%, the highest among all baselines. In contrast, the BC and BC+ approaches perform particularly poorly. We attribute this to the compounding errors effect and the inherent inability of BC methods to generalize from a small training set.

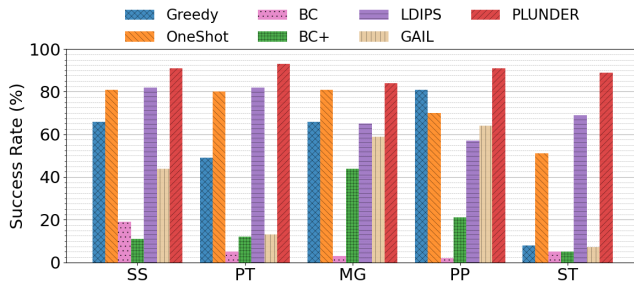


Fig. 8: Success Rates

#### D. Convergence

Our experiments support our hypothesis that the accuracy of the synthesized policies increases with each iteration of the EM loop. PLUNDER converges to a policy across all tasks in fewer than 10 iterations. For instance, Figure 9 illustrates the performance of the synthesized policy after each EM loop iteration for the SS and ST tasks.

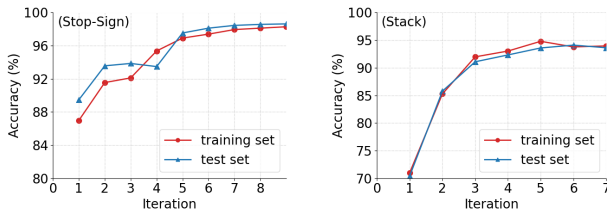


Fig. 9: The progress of the EM loop until convergence in SS (left) and ST (right) tasks.

#### E. Impact of Noise

We evaluate the performance of each baseline as we vary the amount of actuation noise in the training data for the MG task. The accuracies and observation log likelihoods of

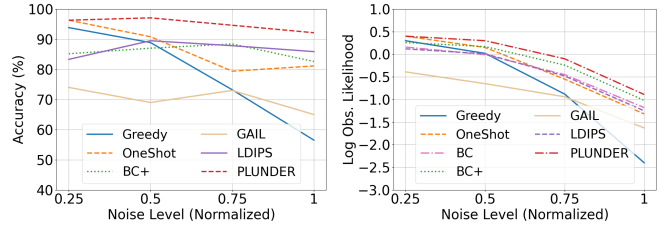


Fig. 10: Impact of noise on performance.

the trajectories produced by all methods are depicted in Figure 10. All approaches show a decrease in performance as the noise increases; however, PLUNDER consistently surpasses other baselines, indicating its superior robustness against noise. We also note that OneShot is more robust against noise compared to Greedy. This underscores the significance of employing a particle filter, even when backed by a simplistic prior. Lastly, the results indicate that BC+ has an advantage over BC, hinting that having access to the observation model provides useful inductive bias that helps overcome the noise in the data.

#### F. Qualitative Analysis

We found that in all tasks, the synthesized programs contain non-trivial conditions that require multiple incremental synthesis steps to be discovered. For instance, the following transition condition was synthesized in the PT task:

$$\begin{aligned} \phi_{\text{FASTER,LANELEFT}} &= \text{flp}(\text{lgs}(x - f_x, -30.62, 1.78)) \\ &\wedge \text{flp}(\text{lgs}(f_x - l_x, -4.92, -6.53)) \\ &\wedge \text{flp}(\text{lgs}(r_x - l_x, 2.95, -1.67)) \end{aligned}$$

The expression above accurately reflects the behaviors observed in the demonstrations. It states: “If the vehicle’s position ( $x$ ) is approaching the position of the vehicle in front ( $f_x$ ), and the position of the vehicle to the left ( $l_x$ ) is farther away than both the vehicle in front and the position of the vehicle to the right ( $r_x$ ), then switch to the left lane”. Such expressions are amenable to repair and formal verification, which is a significant advantage of PLUNDER over methods such as BC, BC+, and GAIL. Note that expressions of this complexity exceed the capabilities of naïve enumeration techniques, which would need to optimize real-valued parameters across more than a billion sketches to identify such a policy. Such enumeration would not be feasible within an EM loop.

## V. RELATED WORK

**Imitation Learning:** Imitation Learning (IL) provides a promising framework for learning autonomous agent behaviors from human demonstrations [1]. Unlike Reinforcement Learning (RL), IL does not require explicit reward signals. Although RL has been successful in addressing numerous complex tasks [22], [23], IL techniques are better suited for many domains where formulating effective reward objectives proves extremely challenging [24].

Within the broad umbrella of IL techniques, Behavior Cloning (BC) and Inverse Reinforcement Learning (IRL) have gained notable attention. BC focuses on establishing

a function that directly associates observations with actions [25], [26], [27]. In contrast, IRL aims to decode the intrinsic reward structure from the given trajectories and subsequently leverages RL for policy inference [28], [29]. IRL typically demands more sophisticated algorithms and a substantial amount of training data to infer the expert’s inherent motivations. Its primary objective is to *enhance* the expert’s performance or *transfer* the acquired knowledge to related tasks [30]. In contrast, our approach in PLUNDER aligns more closely with the BC setup, where a rapid and precise replication of expert behaviors is needed, and access to a complete simulation of the system is not available.

The Generative Adversarial Imitation Learning (GAIL) approach is a widely recognized IL technique that draws insight from both BC and IRL [20]. GAIL concurrently trains a policy network and a discriminator network through an adversarial mechanism [21], and has shown superior performance, particularly in large, high-dimensional environments. However, the neural policies trained by GAIL are not interpretable or repairable, and as such, it does not effectively address the PIL problem solved by PLUNDER. Furthermore, GAIL requires a complete simulation of the system, while PLUNDER necessitates only an observation model, which is often more accessible in practice [31].

**Interpretable Policy Learning:** There is a growing interest in machine learning methodologies with enhanced *interpretability* [32], meaning that the learned models can be represented using programmatic and human-readable structures like decision trees [5] and finite-state machines [33], [34]. For sequential decision-making tasks too, programmatic policy inference has been studied under both reinforcement learning and imitation learning settings [35].

In the RL setting, traditional gradient-driven methods such as DDPG and PPO have been employed to train a neural oracle, that is subsequently used for deriving a programmatic policy. Notably, NDPS [36] and PROPEL [37] utilize domain-specific context-free grammars to define the space of programmatic policies, and employ program synthesis to find the program within that space which best mimics the neural oracle. Another interpretable RL technique is presented by Qiu et. al [38], which concurrently learns program structures and parameters through a differentiable domain-specific language, obviating the initial neural oracle training. Note that all the above strategies are designed for RL and rely on reward signals to learn a policy.

There are also multiple approaches for programmatic policy inference under the IL setting [39], [2], [40]. For instance, LDIPS [2] is a recent IL method that attempts to synthesize programmatic policies from human demonstrations. Similar to PLUNDER, LDIPS uses a domain-specific language to enumerate program sketches, but it relies on a Satisfiability Modulo Theories (SMT) solver to find sketch completions. Moreover, LDIPS requires access to action labels and only synthesizes deterministic policies incapable of reasoning about noise in the demonstrations. This leads to lower performance, as shown by our experiments.

Another notable IL approach offering a degree of inter-

pretability is an extension of GAIL called InfoGAIL [40]. InfoGAIL conducts unsupervised clustering of the provided demonstrations to identify latent *modes* of behavior within expert demonstrations and then infers a distinct policy for each mode. However, InfoGAIL necessitates prior knowledge of the number of modes and their distribution, and the derived policies for each mode are still represented by an opaque neural network. In contrast, PLUNDER’s policies are fully interpretable and accurately explain the noise distribution at decision boundaries in the given demonstrations.

**Offline Policy Learning:** A significant advantage of PLUNDER over many existing IL methodologies [20], [41], [40] is its fully *offline* learning capability. Offline policy learning is often favored over its online counterparts because executing intermediate policies in simulation or the real world is usually slow, costly, and potentially hazardous [42]. Additionally, offline learning enables usage of historical datasets, thereby enhancing the method’s applicability.

There are approaches that conduct IL in a fully offline manner. For instance, ORIL [43] adapts the GAIL framework for offline settings and learns a policy using a collection of logged experiences and expert demonstrations. ORIL first learns a reward model by contrasting the expert demonstrations and the logged experiences, and uses it to learn a policy via offline RL [44]. However, ORIL demands hundreds of expert demonstrations and many thousands of logged experiences, while also training an opaque neural policy. In comparison, PLUNDER needs fewer than a dozen trajectories and produces a fully interpretable policy.

**Expectation Maximization Techniques:** The Expectation Maximization (EM) algorithm is a commonly used technique in situations where both the generative model and its hidden states are unknown [6]. Recently, EM has been applied in various robotics domains. For example, in [45], the authors propose using an EM loop to simultaneously learn a dynamics model and estimate the robot’s state trajectories. In [46], an internal EM loop was employed to optimize a learned policy. However, this method is focused on reinforcement learning and is not well-suited for handling noise. In contrast, our approach leverages an EM loop to infer action labels from noisy demonstrations, while concurrently synthesizing a complex probabilistic program to maximize the likelihood of the demonstration.

## VI. CONCLUSIONS AND FUTURE WORK

We presented PLUNDER, an algorithm for inferring probabilistic action selection policies from noisy and unlabeled demonstrations. A reusable implementation of PLUNDER, as well as all empirical evaluation results comparing our approach to multiple state-of-the-art baselines, is available online. In future work, we aim to minimize the required user input by optimizing the observation model concurrently. Additionally, we plan to explore other advanced synthesis techniques, such as those utilizing Large Language Models [47], within the context of the EM loop to further enhance the usability of this approach.

## REFERENCES

- [1] B. Zheng, S. Verma, J. Zhou, I. W. Tsang, and F. Chen, "Imitation learning: Progress, taxonomies and challenges," *IEEE Transactions on Neural Networks and Learning Systems*, pp. 1–16, 2022.
- [2] J. Holtz, A. Guha, and J. Biswas, "Robot action selection learning via layered dimension informed program synthesis," in *Conference on Robot Learning*, pp. 1471–1480, 2020.
- [3] J. R. Marino, R. O. Moraes, T. C. Oliveira, C. Toledo, and L. H. Lelis, "Programmatic strategies for real-time strategy games," in *Proceedings of the AAAI Conference on Artificial Intelligence*, vol. 35, pp. 381–389, 2021.
- [4] L. C. Medeiros, D. S. Aleixo, and L. H. Lelis, "What can we learn even from the weakest? learning sketches for programmatic strategies," in *Proceedings of the AAAI Conference on Artificial Intelligence*, vol. 36, pp. 7761–7769, 2022.
- [5] S. Orfanos and L. H. Lelis, "Synthesizing programmatic policies with actor-critic algorithms and relu networks," *arXiv preprint arXiv:2308.02729*, 2023.
- [6] R. M. Neal and G. E. Hinton, *A View of the EM Algorithm that Justifies Incremental, Sparse, and other Variants*, pp. 355–368. Dordrecht: Springer Netherlands, 1998.
- [7] A. G. Cunningham, E. Galceran, R. M. Eustice, and E. Olson, "Mpdm: Multipolicy decision-making in dynamic, uncertain environments for autonomous driving," in *2015 IEEE International Conference on Robotics and Automation (ICRA)*, pp. 1670–1677, 2015.
- [8] R. S. Sutton, D. Precup, and S. Singh, "Between mdps and semi-mdps: A framework for temporal abstraction in reinforcement learning," *Artificial Intelligence*, vol. 112, no. 1, pp. 181–211, 1999.
- [9] A. Pfeffer, *Practical probabilistic programming*. Simon and Schuster, 2016.
- [10] S. Thrun, "Probabilistic robotics," *Communications of the ACM*, vol. 45, no. 3, pp. 52–57, 2002.
- [11] A. Doucet, N. De Freitas, N. J. Gordon, et al., *Sequential Monte Carlo methods in practice*, vol. 1. Springer, 2001.
- [12] A. Doucet, A. M. Johansen, et al., "A tutorial on particle filtering and smoothing: Fifteen years later," *Handbook of nonlinear filtering*, vol. 12, no. 656–704, p. 3, 2009.
- [13] S. Gulwani, O. Polozov, and R. Singh, "Program synthesis," vol. 4, pp. 1–119, 2017.
- [14] A. Solar-Lezama, *Program synthesis by sketching*. Citeseer, 2008.
- [15] D. C. Liu and J. Nocedal, "On the limited memory bfgs method for large scale optimization," *Mathematical programming*, vol. 45, no. 1-3, pp. 503–528, 1989.
- [16] J. Holtz, A. Guha, and J. Biswas, "Interactive robot transition repair with smt," in *International Joint Conference on Artificial Intelligence (IJCAI)*, pp. 4905–4911, 2018.
- [17] E. Leurent, "An environment for autonomous driving decision-making." <https://github.com/eleurent/highway-env>, Accessed March 2023.
- [18] Q. Gallouédec, N. Cazin, E. Dellandréa, and L. Chen, "panda-gym: Open-Source Goal-Conditioned Environments for Robotic Learning," *4th Robot Learning Workshop: Self-Supervised and Lifelong Learning at NeurIPS*, 2021.
- [19] A. O. Ly and M. Akhloufi, "Learning to drive by imitation: An overview of deep behavior cloning methods," *IEEE Transactions on Intelligent Vehicles*, vol. 6, no. 2, pp. 195–209, 2021.
- [20] J. Ho and S. Ermon, "Generative adversarial imitation learning," in *Advances in Neural Information Processing Systems* (D. Lee, M. Sugiyama, U. Luxburg, I. Guyon, and R. Garnett, eds.), vol. 29, Curran Associates, Inc., 2016.
- [21] I. Goodfellow, J. Pouget-Abadie, M. Mirza, B. Xu, D. Warde-Farley, S. Ozair, A. Courville, and Y. Bengio, "Generative adversarial nets," *Advances in neural information processing systems*, vol. 27, 2014.
- [22] D. Silver, J. Schrittwieser, K. Simonyan, I. Antonoglou, A. Huang, A. Guez, T. Hubert, L. Baker, M. Lai, A. Bolton, et al., "Mastering the game of go without human knowledge," *nature*, vol. 550, no. 7676, pp. 354–359, 2017.
- [23] R. S. Sutton and A. G. Barto, *Reinforcement learning: An introduction*. MIT press, 2018.
- [24] A. Boularias, J. Kober, and J. Peters, "Relative entropy inverse reinforcement learning," in *Proceedings of the fourteenth international conference on artificial intelligence and statistics*, pp. 182–189, JMLR Workshop and Conference Proceedings, 2011.
- [25] S. Ross, G. Gordon, and D. Bagnell, "A reduction of imitation learning and structured prediction to no-regret online learning," in *Proceedings of the fourteenth international conference on artificial intelligence and statistics*, pp. 627–635, JMLR Workshop and Conference Proceedings, 2011.
- [26] S. Daftary, J. A. Bagnell, and M. Hebert, "Learning transferable policies for monocular reactive mav control," in *2016 International Symposium on Experimental Robotics*, pp. 3–11, Springer, 2017.
- [27] M. Bojarski, D. Del Testa, D. Dworakowski, B. Firner, B. Flepp, P. Goyal, L. D. Jackel, M. Monfort, U. Muller, J. Zhang, et al., "End to end learning for self-driving cars," *arXiv preprint arXiv:1604.07316*, 2016.
- [28] B. D. Ziebart, A. Maas, J. A. Bagnell, and A. K. Dey, "Maximum entropy inverse reinforcement learning," in *Proc. AAAI*, pp. 1433–1438, 2008.
- [29] P. Abbeel and A. Y. Ng, "Apprenticeship learning via inverse reinforcement learning," in *Proceedings of the twenty-first international conference on Machine learning*, p. 1, 2004.
- [30] D. Brown, W. Goo, P. Nagarajan, and S. Niekum, "Extrapolating beyond suboptimal demonstrations via inverse reinforcement learning from observations," in *International conference on machine learning*, pp. 783–792, PMLR, 2019.
- [31] L. Ljung, "System identification," in *Signal analysis and prediction*, pp. 163–173, Springer, 1998.
- [32] C. Molnar, *Interpretable machine learning*. Lulu. com, 2020.
- [33] J. P. Inala, O. Bastani, Z. Tavares, and A. Solar-Lezama, "Synthesizing programmatic policies that inductively generalize," in *International Conference on Learning Representations*, 2019.
- [34] D. Trivedi, J. Zhang, S.-H. Sun, and J. J. Lim, "Learning to synthesize programs as interpretable and generalizable policies," in *Advances in Neural Information Processing Systems* (M. Ranzato, A. Beygelzimer, Y. Dauphin, P. Liang, and J. W. Vaughan, eds.), vol. 34, pp. 25146–25163, Curran Associates, Inc., 2021.
- [35] N. Topin and M. Veloso, "Generation of policy-level explanations for reinforcement learning," in *Proceedings of the AAAI Conference on Artificial Intelligence*, vol. 33, pp. 2514–2521, 2019.
- [36] A. Verma, V. Murali, R. Singh, P. Kohli, and S. Chaudhuri, "Programmatically interpretable reinforcement learning," in *International Conference on Machine Learning*, pp. 5045–5054, PMLR, 2018.
- [37] A. Verma, H. Le, Y. Yue, and S. Chaudhuri, "Imitation-projected programmatic reinforcement learning," *Advances in Neural Information Processing Systems*, vol. 32, 2019.
- [38] W. Qiu and H. Zhu, "Programmatic reinforcement learning without oracles," in *International Conference on Learning Representations*, 2022.
- [39] S. Teng, L. Chen, Y. Ai, Y. Zhou, Z. Xuanyuan, and X. Hu, "Hierarchical interpretable imitation learning for end-to-end autonomous driving," *IEEE Transactions on Intelligent Vehicles*, vol. 8, no. 1, pp. 673–683, 2023.
- [40] Y. Li, J. Song, and S. Ermon, "Infogail: Interpretable imitation learning from visual demonstrations," *Advances in neural information processing systems*, vol. 30, 2017.
- [41] T. Osa, J. Pajarinen, G. Neumann, J. A. Bagnell, P. Abbeel, J. Peters, et al., "An algorithmic perspective on imitation learning," *Foundations and Trends® in Robotics*, vol. 7, no. 1-2, pp. 1–179, 2018.
- [42] A. J. Chan and M. van der Schaar, "Scalable bayesian inverse reinforcement learning," *arXiv preprint arXiv:2102.06483*, 2021.
- [43] K. Zolna, A. Novikov, K. Konyushkova, C. Gulcehre, Z. Wang, Y. Ayar, M. Denil, N. de Freitas, and S. Reed, "Offline learning from demonstrations and unlabeled experience," *arXiv preprint arXiv:2011.13885*, 2020.
- [44] R. Rafailov, T. Yu, A. Rajeswaran, and C. Finn, "Offline reinforcement learning from images with latent space models," in *Learning for Dynamics and Control*, pp. 1154–1168, PMLR, 2021.
- [45] J. Wei, J. Holtz, I. Dillig, and J. Biswas, "STEADY: Simultaneous state estimation and dynamics learning from indirect observations," in *Intelligent Robots and Systems (IROS), IEEE/RSJ International Conference on, IEEE*, 2022.
- [46] J. P. Inala, O. Bastani, Z. Tavares, and A. Solar-Lezama, "Synthesizing programmatic policies that inductively generalize," in *International Conference on Learning Representations*, 2020.
- [47] N. Patton, K. Rahmani, M. Missula, J. Biswas, and I. Dillig, "Program synthesis for robot learning from demonstrations," 2023.